Eur. Phys. J. B **26**, 51–55 (2002)
DOI: 10.1140/epjb/e20020065

THE EUROPEAN PHYSICAL JOURNAL B
EDP Sciences

Crystal structure and morphology of the $NdSr_2RuCu_2O_y$ compound

A. Vecchione[1], M. Gombos[1], S. Pace[1], L. Marchese[2], G. Cerrato[3], C. Tedesco[4], P.W. Stephens[5], and C. Noce[1,a]

[1] Unità I.N.F.M. di Salerno, Dipartimento di Fisica "E.R. Caianiello", Università di Salerno, 84081 Baronissi (Salerno), Italy
[2] Dipartimento di Scienze e Tecnologie Avanzate, Università del Piemonte Orientale "A. Avogadro", 15100 Alessandria, Italy
[3] Dipartimento di Chimica I.F.M., Università di Torino, 10125 Torino, Italy
[4] Dipartimento di Chimica, Università di Salerno, 84081 Baronissi (Salerno), Italy
[5] NSLS, Brookhaven National Laboratory, Upton, NY 11973, USA & Dept. of Physics and Astronomy, State University of New York, Stony Brook, NY 11974-3800, USA

Received 15 November 2001

Abstract. We report the preparation and the structural and morphological characterization of the perovskite compound $NdSr_2RuCu_2O_y$. The crystal structure of this material has been determined by a combined high-resolution electron microscopy, selected area electron diffraction and high-resolution X-ray powder diffraction study. The morphology of the samples has been monitored by a scanning electron microscope equipped with an energy dispersive spectrometer attachment by which the microanalysis of the crystallites has been also performed. Finally, dc magnetic susceptibility measurements show that this compound behaves like an enhanced paramagnetic metal with evidence of neither magnetic order and neither superconducting one.

PACS. 61.66.-f Structure of specific crystalline solids – 61.10.Nz Single crystal and powder diffraction – 68.37.-d Microscopy of surfaces, interfaces, and thin films

1 Introduction

One of the most important developments associated with the discovery of high temperature superconductivity in the cuprates has been a rapid growth in our understanding of related oxides. Oxides display all the ground states of strongly correlated electron physics, from many-body insulators to metals on the border of applicability of the well-known Fermi liquid theory. The various forms of magnetism which also occur are linked to a host of interesting properties such as colossal magnetoresistance and unconventional superconductivity. Recently, the class of ruthenate materials has been the focus of considerable work because of their interesting magnetic and superconducting properties. $SrRuO_3$ is a band ferromagnet [1]; Sr_2RuO_4 is an exotic p-wave superconductor [2]; $RuSr_2GdCu_2O_8$ [3] exhibits a coexistence of bulk superconductivity and uniform magnetic ordering. In this hybrid ruthenate-cuprate system both the Cu-O and Ru-O planes form very similar square-planar arrays, and the coexistence of superconductivity and long range magnetic order is intriguing [4]. However, in spite of extensive investigation a consistent picture of the magnetic structure is still lacking [5,6]. Other compounds of the type $RuSr_2RE_{2-x}Ce_xCu_2O_{10}$ and $RuSr_2RECu_2O_8$ (hereafter named 1212 compounds), with RE=Sm, Eu were synthesized in early 1995 [7] and some of them exhibit the coexistence of superconductivity and magnetic order [8,9].

The fact that materials closely linked both chemically and structurally may show largely different physical properties may give a unique opportunity to tackle correlated electron physics with controlled material parameters. Therefore, the synthesis of a wider group of materials of the 1212 class can be considered a key objective, though attempts to synthesize other than Gd, Eu RE-based 1212 rutheno-cuprate systems have not been so far successful. Indeed, Tallon and co-workers [10] found that, beside $RuSr_2GdCu_2O_8$, $RuSr_2SmCu_2O_8$ could be also made, though this phase represents only a small ($\sim 20\%$) fraction of the whole sample. Tang *et al.* reported attempts to synthesize $NdSr_2RuCu_2O_y$ but the presence of Nd ions in the 1212 structure was limited and a segregation of $SrRuO_3$ phase was observed [11]. Bauernfeind *et al.* proposed that the formation of the 1212 phase depends on the ionic radius of rare-earth, and the fact that neodymium has an ionic radius larger than the one of samarium and europium, led to the formation of a mixture of perovskites of unknown stoichiometry [7]. For completeness, it is worth noticing that very recently a new rutheno-cuprate oxide has been synthesized in which Gd is replaced by Y, and it

[a] e-mail: canio@sa.infn.it

is found that a superconducting gap coexists with a ferromagnetic component at a microscopic level below the temperature of the onset of superconductivity [12].

In this paper we report the preparation and the structural characterization of the Nd-based rutheno-cuprate perovskite-type material. Crystal structure and morphology of this microcrystalline material were obtained by a study combining high-resolution X-ray powder diffraction, scanning electron microscopy (SEM), high-resolution transmission electron microscopy (HRTEM) and selected area electron diffraction (SAED) which provide clear-cut evidences of the formation of this perovskite structure. Finally, in order to study the role played by Nd ions on magnetic properties of $NdSr_2RuCu_2O_y$ we report the dc magnetic susceptibility of Nd-based 1212 compound as well as the experimental results obtained for $GdSr_2RuCu_2O_x$ material.

2 Experimental

Samples of $NdSr_2RuCu_2O_y$ and $RuSr_2GdCu_2O_x$ were obtained by solid state reaction of a mixture of stoichiometric powders of high purity RuO_2, Nd_2O_3, Gd_2O_3, CuO oxides and strontium carbonate ($SrCO_3$). The powders were decomposed in alumina crucibles by heating at 5 °C/min up to 960 °C and held at this temperature for 10 hours in air and subsequently cooled to room temperature. This step is crucial to produce the desired phase. These powders were ground and milled before reaction at 1000 °C for 10 hours in flowing nitrogen. This step was necessary to limit the formation of $SrRuO_3$ [7]. Finally, the powders were annealed with a procedure made by several cycles of heating at temperatures ranging from 1050 °C to 1080 °C and subsequent cooling at room temperature in pure oxygen atmosphere. The phases produced after each step were routinely monitored by X-ray powder diffraction (XRPD). XRPD patterns were obtained on a Philips PW-1700 diffractometer using Ni-filtered CuKα radiation. Diffraction patterns were collected at room temperature over the 2θ range 5°–100° with a step size of 0.05° and time per step of 20 seconds.

High-resolution X-ray powder diffraction data were recorded at room temperature in transmission geometry at NSLS beamline X3B1, Brookhaven National Laboratory. The sample was sealed in a 0.5 mm Lindemann capillary and was spun during measurements in order to improve randomization of the crystallites. The diffracted beam is analyzed by a Ge(111) crystal placed before a NaI scintillation counter. In this parallel beam configuration, the resolution is determined by the analyzer crystal instead of by slits [13]. A 0.40174(2) Å wavelength was selected in order to minimize absorption. Data were collected from 1.000° to 32.954° 2θ using a step size of 0.002° and step time of 3 s and then normalized against monitor counts. Rietveld refinement was performed using the program GSAS [14]. The peak profile was described by a pseudo Voigt function [15], in combination with a special function that accounts for the asymmetry due to axial divergence [16].

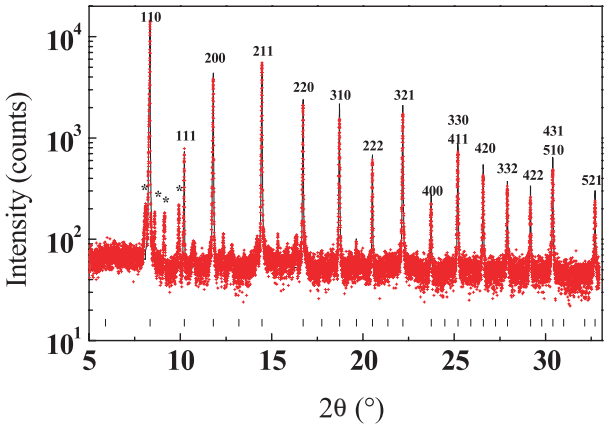

Fig. 1. High resolution X-ray powder diffraction pattern of an oxygen annealed sample of $NdSr_2RuCu_2O_y$ together with the best-fit Rietveld profile. Observed profile points are indicated by (+), Bragg peak positions are marked as vertical bars, peaks marked by stars are due to phase impurities.

Thermal analysis (TGA/DTA) was carried out on a TA instrument (SDT2960 model) by keeping 10-15 mg of sample under a constant flux of air and at 5 °C/min heating rate up to 1000 °C. The morphology of the crystalline powders was analyzed by scanning electron microscopy on a Leica Stereoscan 420. This microscope was equipped with an energy dispersive spectrometer (EDS) attachment, by which elemental chemical analysis of selected areas of the sample (<1 μm^2) was performed. High-resolution transmission electron microscopic images and selected area electron diffraction patterns were obtained by a Jeol JEM 2000-EX instrument which allowed to get a structural characterization of micro-crystallites. The HRTEM microscope was equipped with a top-entry stage, LaB_6 filament, and operating at 200 kV-acceleration voltage. All samples in form of powder were first dispersed in n-heptane, then a drop of the suspension was put on a "holey" carbon-coated Cu grid (200 mesh). Dc susceptibility measurements were performed by means of an Oxford Maglab Vibrating Sample Magnetometer (VSM). The samples vibrate in a region where the magnetic field homogeneity is equal to one part per million. All measurements were performed after sieving the materials and collecting the fraction with size smaller than 5 μm.

3 Results and discussion

High resolution X-ray powder diffraction pattern of an oxygen annealed sample of $NdSr_2RuCu_2O_y$ is shown in Figure 1. Reflections marked by stars are due to small amounts of extra-phase, not included in the Rietveld analysis. The diffraction pattern was successfully indexed assuming a cubic cell with lattice parameter $a = 3.91$ Å, this value was refined later to $a = 3.90727(3)$ Å by Rietveld refinement in $Pm\overline{3}m$ space group.

The cubic symmetry, as unambiguously assessed in the indexing procedure, requires the presence of disorder

Table 1. Atomic parameters for $NdSr_2RuCu_2O_y$ resulted from the Rietveld refinement, $Pm\overline{3}m$ a = 3.90727(3) Å. R_p = 0.1536, $R_{wp} = 0.2060$, $R_{F^2} = 0.090$.

	x	y	z	U_{11}	Occ.
Ru	0	0	0	0.0065(4)	0.33
Cu	0	0	0	0.0065(4)	0.67
Nd	0.5	0.5	0.5	0.0228(5)	0.33
Sr	0.5	0.5	0.5	0.0228(5)	0.67
O(1)	0.0	0	0.25	0.053(2)	1.00

between cation sites. This type of positional disorder affects both perovskite A and B cation sites.

Various types of disorder were modelled by the Rietveld refinement, best results were obtained assuming that the perovskite A sites can be occupied either by Nd or Sr cations and B sites by either Ru or Cu. No satisfactory result was obtained allowing different substitutions. In agreement with EDS measurements, good convergence was achieved assuming a 1:2 ratio both between Nd:Sr and Ru:Cu cations as listed in Table 1, where also the final results of Rietveld refinement are reported. In spite of the small difference between ionic radii of Nd^{3+} and Gd^{3+} (0.03 Å) the structure of homologous rutheno-cuprates show significant differences. In the first case a disordered cubic perovskite structure is formed, while in the latter case an ordered triple perovskite structure is obtained. This is in agreement with results already reported in the literature, where the formation of an ordered 1212 phase seems strongly influenced on the size of the lanthanide. Bauernfeind *et al.* [7] observed that lanthanide cations with radius larger than Sm appear to prefer substitution on Sr sites, while lanthanides smaller than Gd form preferably the ordered double perovskite $Sr_2(LnRu)O_6$. Moreover, Nd ions show an higher tendency than Gd ions for substitution on earth-alkaline ion sites as observed in rare-earth cuprate superconductors [17].

On the other hand, the formation of an ordered 1212 phase with Pr has been recently reported [18]. This suggests that also other factors besides lanthanide ion radius must be taken into account, as for example the ratio between the radius of various cations.

The absence of contamination from both alumina crucibles and other spurious elements is checked by EDS analysis of a large area of the samples (200×200 μm^2) that shows only the presence of the elements of the starting materials. Figure 2 shows a SEM micrograph of $NdSr_2RuCu_2O_y$, which is constituted by aggregates of crystallites of tens of microns. An inspection of these aggregates at higher magnification shows that they are composed by submicrometer particles of average size down to 0.5 μm. A quantitative EDS analysis performed on several points of the sample confirms that these aggregates are $NdSr_2RuCu_2O_y$ phase.

Although to a lesser extent, small regions with Nd deficiency are also detected. These are associated with the formation of strontium oxide, the amount of which is too low to be revealed by XRD. Figure 3 shows a low magnification

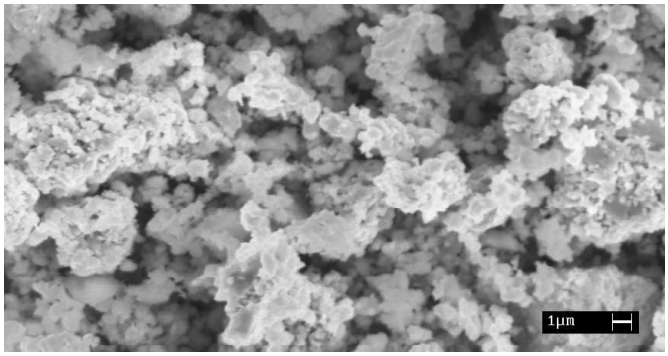

Fig. 2. SEM image of $RuSr_2NdCu_2O_y$.

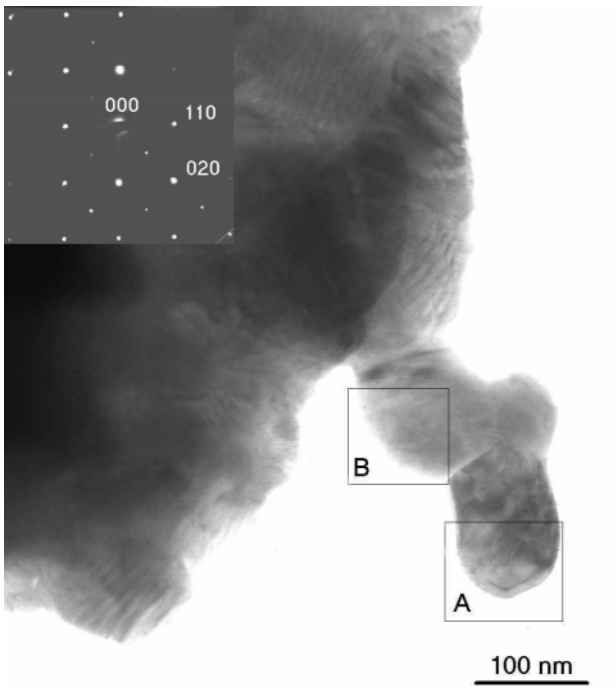

Fig. 3. TEM micrograph showing a large aggregate of $NdSr_2RuCu_2O_y$. The inset shows a SAED pattern from the region A where a single microcrystal is oriented down to the [001] direction. The main diffraction spots belong to (110) and (020) planes, and weaker spots of (010) planes are also observable. Region B shows another single particle which was studied by HRTEM (see Fig. 4).

image of a more detailed morphological analysis of the particles forming the aggregates performed by TEM. Domains with different extension of sintering between particles are evident in these large areas. Moreover, the particles protruding from large aggregates result mainly round-shaped and with average size of 100–150 nm. These particles are ideal for both SAED and HRTEM analyses. The inset of Figure 3 shows a SAED pattern of the region A where a single microcrystal is found. The particle is oriented down to the [001] direction and the main diffraction spots are measured at 1.92 Å and 2.71 Å corresponding respectively

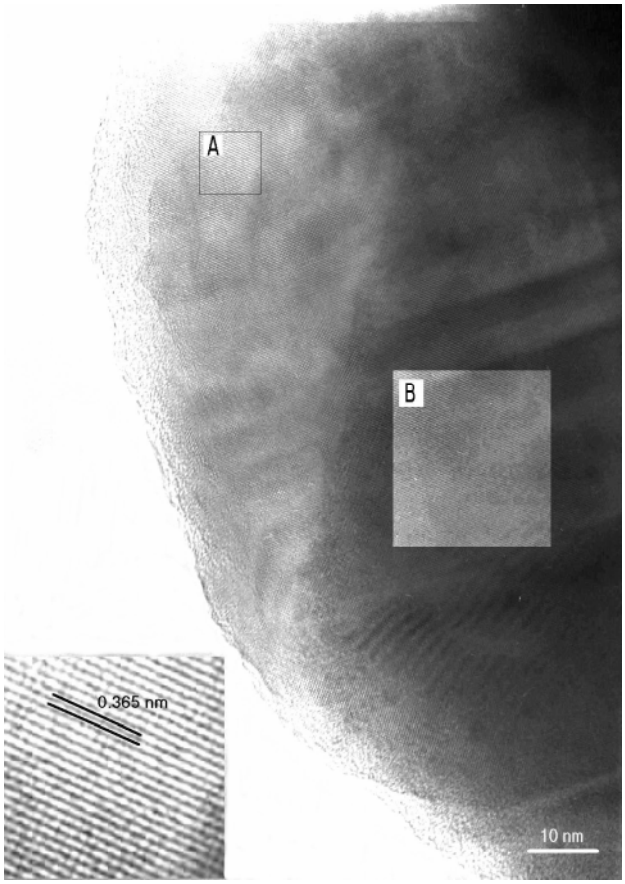

Fig. 4. HRTEM image of a single microcrystal of $NdSr_2RuCu_2O_y$. The inset shows an enlarged view of the region A where lattice fringes 3.65 Å apart from (100) planes are visible. Region B is an enlightened part of the microcrystal where regular lattice fringes of (100) planes are also found.

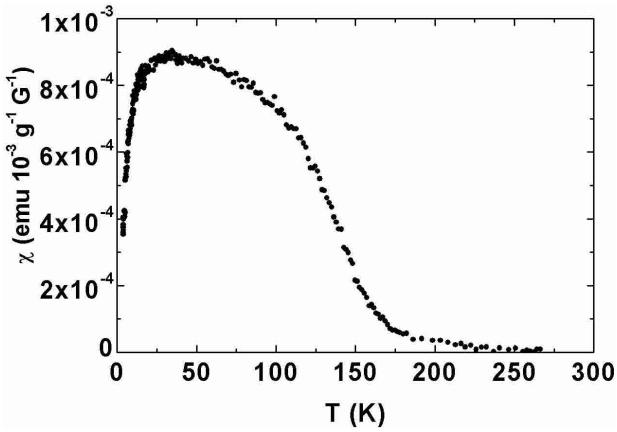

Fig. 5. dc magnetic susceptibility for $RuSr_2GdCu_2O_x$.

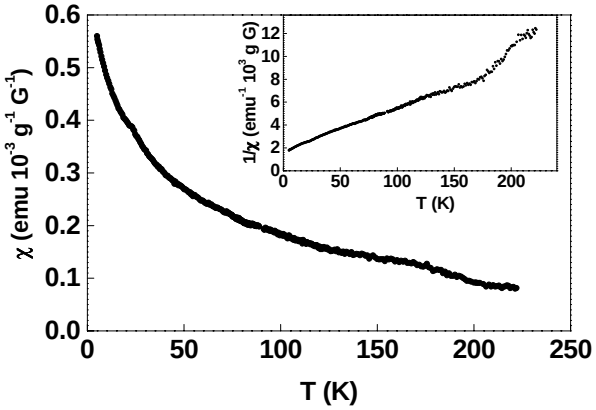

Fig. 6. dc magnetic susceptibility for $NdSr_2RuCu_2O_y$. In the inset is reported the inverse magnetic susceptibility as a function of the temperature.

to (020) and (110) planes of a cubic unit cell of 1212-type $RuSr_2NdCu_2O_8$ phase. Figure 4 shows a HRTEM image (region B of Fig. 3), where lattice fringes 3.65 Å apart are found, and these could be assigned to (100) planes of a the 1212-type $NdSr_2RuCu_2O_y$ phase (see the inset of Fig. 4 which reports an enlargement view of the region A). Large domains (200–300 Å^2) where the lattice fringes of (100) planes extend regularly (see for instance the region B in Fig. 4) are found in many particles and suggest that large areas of the microcrystals have regular bulk structure. Besides regular domains, there are also regions where lattice fringes interrupt frequently which suggests that the particles have an irregular (stepped) morphology as well as extended defects, such as stacking faults. Areas of individual domains are also observed, particularly along the border of the particles. These domains are much smaller than those enlightened in region B.

Figures 5 and 6 present the temperature dependencies of the dc susceptibility in a small external magnetic field (1G), for $RuSr_2GdCu_2O_x$ and $NdSr_2RuCu_2O_y$ compounds respectively.

The main features observed in Figure 5 are (i) the decrease in the susceptibility below 30 K, (ii) the increase of the same quantity for temperature below ∼150 K. We first discuss the decrease in the susceptibility for temperatures below 30 K. A similar decrease was observed in other similar compound, namely in $RuSr_2EuCu_2O_8$ below 32 K; in $Eu_{1.4}Ce_{0.6}RuSr_2Cu_2O_{10-\delta}$ below 32 K and in $Gd_{1.4}Ce_{0.6}RuSr_2Cu_2O_{10-\delta}$ below 42 K. It has been argued that this feature is due to the appearance of superconductivity, where the bulk Meissner phase is suppressed due to granularity or spontaneous vortex phase [9]. We now consider the increase of the susceptibility below ∼150 K. The sudden onset of the susceptibility indicates a ferromagnetic transition and this result is also supported by an irreversible behavior in the $M(H)$ loop. Nevertheless, neutron powder-diffraction shows that below the magnetic ordering temperature, this compound has a G-type antiferromagnetic structure in which Ru moments are antiparallel in all three crystallographic directions. The ferromagnetism in this compound, which is clearly indicated by the susceptibility measurements as well as by hysteresis loops, can be explained if the Ru moments are canted to give a net moment perpendicular to the c axis [20].

On the contrary, the data presented in Figure 6 for $NdSr_2RuCu_2O_y$ sample indicate that there is no signature of both the magnetic and superconducting transition. Indeed, this compound exhibits a paramagnetic behavior well described in terms of Curie law below 150 K (see the Inset in Fig. 6). For completeness, we notice that the vertical scales in Figures 5 and 6 are different and this corresponds to a low temperature susceptibility for the $NdSr_2RuCu_2O_y$ about two order of magnitude larger than the one for the $GdSr_2RuCu_2O_y$ compound. Two main reasons could be considered to explain the experimental data. Firstly, the magnetic properties of this compound are dominated by the paramagnetic Nd^{3+} ions and this fact could prevent the magnetic and superconducting transitions. Secondly, the Cu/Ru site mixing as well as between Nd and Sr, suggested by high resolution X-ray powder diffraction and SAED data, further support the absence of any ordered phase in the Nd-based compound. Indeed, this intermixing of cations producing a disordered network of CuO_2 and RuO_2 planes strongly affects the formation of an ordered magnetic structure and inhibits the formation of Cooper pairs in the CuO_2 channel.

4 Summary

In conclusion, we have successfully prepared the perovskite material $NdSr_2RuCu_2O_y$ whose crystal structure and morphology are described by a combination of HRTEM, SAED and SEM/EDS study augmented with high-resolution X-ray powder diffraction analysis. A fair description of the X-ray patterns has been achieved assuming that the main 1212 phase is cubic and the presence of disorder between cations. Besides, the dc magnetic susceptibility exhibits a Curie-Weiss-like behavior with no signature of magnetic transition and neither superconducting instability. The results presented here suggest that the presence of a disordered network of CuO_2 and RuO_2 planes strongly affects the formation of any ordered phase.

National Synchrotron Light Source at Brookhaven National Laboratory is supported by the US Department of Energy, Division of Materials Sciences and Division of Chemical Sciences. The SUNY X3 beamline at NSLS is supported by the Division of Basic Energy Sciences of the US Department of Energy under Grant No. DE-FG02-86ER45231. Financial support by the Italian Ministero dell'Università e della Ricerca Scientifica e Tecnologica (MURST) and the Italian Consiglio Nazionale delle Ricerche (CNR) is gratefully acknowledged. We gratefully acknowledge the contribution of A. Frache for the assistance in SEM and EDS measurements and helpful discussions with Prof A. Immirzi, Dr. M. Cuoco, Dr. A. Romano and Dr. D. Zola.

References

1. J.J. Randall, R. Ward, J. Am. Chem. Soc. **81**, 2629 (1959).
2. Y. Maeno *et al.*, Nature **372**, 532 (1994).
3. C. Bernhard *et al.*, Phys. Rev. B **59**, 14099 (1999).
4. A.C. McLaughlin *et al.*, Phys. Rev. B **60**, 7512 (1999).
5. A. Fainstein *et al.*, Phys. Rev. B **60**, 12597 (1999); A.C. McLaughlin, J.P. Attfield, Phys. Rev. B **60**, 14605 (1999).
6. J.W. Lynn *et al.*, Phys. Rev. B **61**, 14 964 (2000).
7. L. Bauernfeind, W. Widder, H.F. Braun, Physica C **254**, 151 (1995); L. Bauernfeind, W. Widder, H.F. Braun, J. Low Temp. Phys. **105**, 1605 (1996).
8. I. Felner, U. Asaf, Y. Levi, O. Millo, Phys. Rev. B **55**, 3374 (1997); E.B. Sonin, I. Felner, Phys. Rev. B **57**, 14000 (1998); I. Felner, U. Asaf, S. Reich, Y. Tsabba, Physica C **311**, 163 (1999); I. Felner, U. Asaf, Y. Levi, O. Millo, Physica C **334**, 141 (2000).
9. G.V.M. Williams, S. Krämer, Phys. Rev. B **62**, 4132 (2000).
10. J. Tallon *et al.*, IEEE Trans. Appl. Supercond. **9**, 1051 (1999).
11. L.B. Tang *et al.*, Physica C **282-287**, 947 (1997).
12. Y. Tokunaga, H. Kotegawa, K. Ishida, Y. Kitaoka, H. Takagiwa, J. Akimitsu, Phys. Rev. Lett. **86**, 5767 (2001).
13. D.E. Cox, *Handbook of Synchrotron Radiation*, Vol. 3, Chap. 5, *Powder Diffraction*, edited by G. Brown, D.E. Moncton (Elsevier, Amsterdam, 1991).
14. A.C. Larson, R.B. Von Dreele, GSAS - *General Structure Analysis System*, Los Alamos National Laboratory, Los Alamos (USA), LANL Report LAUR 86-748.
15. P. Thompson, D.E. Cox, J.B. Hastings, J. Appl. Cryst. **20**, 79 (1987).
16. L.W. Finger, D.E. Cox, A.P. Jephcoat, J. Appl. Cryst. **27**, 892 (1994).
17. E.A. Goodilin *et al.*, Physica C **272**, 65 (1996); S.I. Yoo, R.W. McCallum, Physica C **210**, 147 (1993).
18. V.P.S. Awana, J. Nakamura, M. Karppinen, H. Yamauchi, S.K. Malik, W.B. Yelon, Physica C **357-360**, 121 (2001).
19. G.V.M. Williams, S. Krämer, Phys. Rev. B **62**, 4132 (2000).
20. J.D. Jorgensen, O. Chmaissem, H. Shaked, S. Short, P.W. Klamut, B. Dabrowski, J.L. Tallon, Phys. Rev. B **63**, 054440 (2001).